Prostate Cancer Shutter-Speed DCE-MRI

Xin Li[1], Ryan A Priest[2,3], William J Woodward[1], Faisal Siddiqui[2,3], Tomasz M Beer[4,5], Mark G Garzotto[6,7], William D Rooney[1], and Charles S Springer[1,5]

[1]Advanced Imaging Research Center, Oregon Health & Science University, Portland, Oregon, United States, [2]School of Medicine, Oregon Health & Science University, Portland, Oregon, United States, [3]Radiology, Oregon Health & Science University, Portland, Oregon, United States, [4]Hematology/Oncology, Oregon Health & Science University, Portland, Oregon, United States, [5]Knight Cancer Institute, Oregon Health & Science University, Portland, Oregon, United States, [6]Urology, Oregon Health & Science University, Portland, Oregon, United States, [7]Portland VA Medical Center, Portland, Oregon, United States

Introduction: For prostate tissue, the extensive and fast contrast reagent (CR) extravasation seen in Dynamic-Contrast-Enhanced MRI (DCE-MRI) data presents a challenge for lesion detection (1). In addition, since extracellular CR and water never distribute equally *in vivo*, water exchange effects become more influential with high interstitial [CR]. Using real data (1-2) and simulations based on region-of-interest (ROI) prostate DCE-MRI, pharmacokinetic parameters extracted from the fast-exchange-limit-constrained (FXL-c) Standard pharmacokinetic modeling (SM) (3), and versions of analytical "shutter-speed" models (SSM) (4) were investigated. The first generation SSM (SSM1) was found sensitive to inter-compartmental water exchange effects. With inclusion of the τ_i (mean intracellular water lifetime) biomarker, the effect on K^{trans} (a CR extravasation rate measure) can be quantified using the difference of its magnitudes returned by sequential SSM1 and SM analyses of a given DCE-MRI time-course.

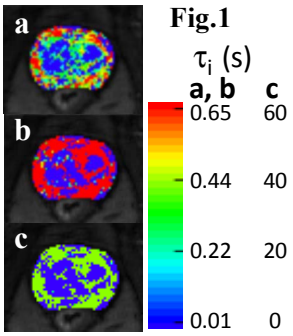

Fig.1

Methods: Prostate ^1H_2O MRI data were acquired from 13 subjects with a Siemens TIM Trio (3T) system under an IRB-approved protocol. RF transmitting was through the whole body coil and RF receiving was with Spine Matrix and flexible Body Matrix coil arrays. The DCE-MRI acquisition employed a 3D FLASH pulse sequence with a 256*144*16 matrix size and a 360*203 mm^2 FOV, resulting in $(1.4)^2$ mm^2 axial-plane resolution. Other parameters are: slice thickness: 3 or 3.2 mm; TR/TE/FA: 5.0 ms/1.57 ms/15º, inter-image sampling interval: 6.3 s. A 0.1 mmol/kg CR (Prohance; Bracco) bolus was administered starting ~30 s after commencing the DCE-MRI sequence. Other details are given in (2). The ROI location had been outlined on a T_2^*-weighted image slice by a radiologist (not involved in DCE-MRI data processing) using hypointensity and morphology criteria. All subjects underwent subsequent standard ten-core prostate biopsies with only ultrasound (US) guidance. A case is benign (eight subjects) from histopathology if no malignancy was found in any of the 10 biopsy core specimens. For positive biopsy specimens, the Gleason scores ranged from 6 to 8 and the number of malignant cores ranged from 1 – 5.

Results: **Figure 1** shows an example testing the results of different pharmacokinetic model constraints with prostate ROI data. Axial τ_i maps for a normal subject from fitting with two SSM versions (4) are shown [(fast-exchange-regime-allowed, FXR-a) and (slow-exchange-regime-allowed, SXR-a) in panels a and b, respectively] with the same color scale. Conspicuous peripheral/central zone (PZ/CZ) contrast is evident in the FXR-a map. Many transitional zone (TZ)/CZ pixels have very small τ_i values - effectively zero in some cases. In the FXR-a map, the τ_i values for a majority of PZ (and possibly fibromuscular stroma) pixels are in the 300-800 ms range: (thus a number of PZ pixels exceed the color scale maximum). The (spatial) correlation with known tissue structure (*i.e.*, the PZ) supports τ_i significance. The SXR-a map in **b** exhibits PZ τ_i values that are uniformly above the color scale maximum. When the latter is raised considerably in **c**, we see that SXR-a returns PZ τ_i values overwhelmingly approaching the upper bound set for the iterative fitting, 40 s, an impossibly large value for prostate parenchymal cell size. These τ_i values are pegged and are just as unreasonable as in the FXL-c where they are held effectively zero. Also, though there is spatial correlation in the (essentially binary) Fig. 1c map, it is not reasonable that all PZ τ_i values be identical; *i.e.*, one does not expect a correct map to be binary. This spatial correlation may imply that the SXR-a/data incompatibility is due to disproportionate signal quenching (5) rather than to a numerical model parameter correlation. The same τ pegging behavior has been observed in human breast tumors (4) and myocardial tissue (6) *in vivo*. Thus, the FXR-a SSM analysis, which represents the essential quenching of the blood and interstitial ^1H_2O signals (4), is more reasonable.

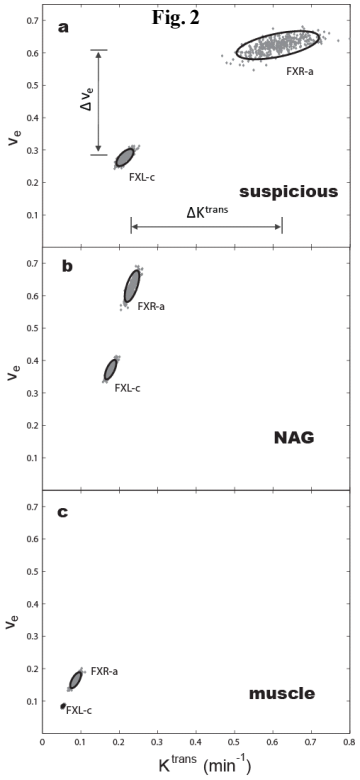

Fig. 2

Figure 2 employs simulations to investigate the usefulness of ΔK^{trans} [$\Delta K^{trans} \equiv K^{trans}$(FXR-a) - K^{trans}(FXL-c)] and parameter correlation/uncertainty in the FXL-c and FXR-a fitting processes. Four hundred simulation runs were carried out for each model on each ROI data set. For this particular case, the suspicious ROI is from the side where all 5 subsequent biopsy specimens showed malignancy ("suspicious" because the pathology was not known when the ROI was chosen). For each simulation run, a new random noise (Gaussian distribution about zero) contribution was added to the time-course data points. This was done so that the simulated data carry no bias from a potential model. Randomly generated initial guess K^{trans}, v_e (extracellular extravascular volume fraction), and τ_i (in FXR-a) values were used for each of the 400 simulated time courses. Each panel shows v_e *vs.* K^{trans} plots: the gray points have the coordinates of the final fitted values - the initial guesses spanned the plot ranges. Two point clusters are shown for each tissue ROI: one for the SM(FXL-c) two parameter [K^{trans} and v_e] fitting, and one for the SSM(FXR-a) three parameter [K^{trans}, v_e, and τ_i] fitting. All panels have the same scales. The two standard deviation (SD) ellipses are also superimposed. In the suspicious prostate tissue (panel a), the difference between the K^{trans} values returned by the SSM(FXR-a) and SM(FXL-c) fittings is large: $\Delta K^{trans} = 0.38$ min^{-1}. It is more than six times larger than for the contralateral normal-appearing-gland (NAG) prostate tissue (panel b), where it is 0.06 min^{-1}. For *obturator* muscle tissue (panel c), the ΔK^{trans} value is even smaller, 0.03 min^{-1}. As far as the effect on the K^{trans} parameter is concerned, the exchange systems in the NAG and muscle tissues remain in, or close to, the FXL condition during most of DCE time-course. This is true despite the fact that the maximum contrast enhancements of NAG and suspicious ROIs are similar (1). The 2SD ellipses show that the ΔK^{trans} parameter is significantly nonzero for the suspicious prostate tissue, and the Δv_e parameter is significantly nonzero for all three tissues. With significantly increased effect size provided by FXR-a and slightly reduced uncertainty [due to systematic error cancelation from the subtraction (7)], the new ΔK^{trans} biomarker could be useful for prostate lesion discrimination. This is particularly encouraging because, with only US guidance here, we know only that the suspicious ROI chosen was on the same side as the malignant needle cores, but not that it was actually penetrated by a needle.

Discussion: The FXR-a analysis gives the physically reasonable results of a larger K^{trans} on the angiogenically malignant side of the prostate, and τ_i values of 300 to 800 ms, while returns the same K^{trans} value (as FXL-c gives) when the CR extravasation concentration is small (*e.g.*, *obturator* muscle), even though τ_i is surely at least as large (5). However, it does this at the expense of assuming effectively complete transverse relaxation quenching of the blood and interstitial ^1H_2O signals. Though this is also reasonable, it cannot be directly ascertained.

Grant Support: Medical Research Foundation of Oregon, NIH: RO1-EB00422, RO1-NS40801.

Reference: **1.** Li, Priest, Siddiqui, Beer, Garzotto, Woodward, Rooney, Springer, *Proc.Int Soc Magn Reson Med*.**17**:4221(2009). **2.** Priest, Li, Tagge, Woodward, Beer, Springer, Garzotto, *Proc.Int Soc Magn Reson Med*. **18**: 2809 (2010). **3.** Tofts, Brix, Buckley, *et al. J Magn Reson Imaging,* **10**:223-232 (1999). **4.** Yankeelov, Rooney, Li, Springer *Magn Reson Med.* **50**:1151-1169 (2003). **5.** Li, Huang, Morris, Tudorica, Seshan, Rooney, Tagge, Wang, Xu, Springer, PNAS, **105**: 17937-17942 (2008). 6. Li, Springer, Jerosch-Herold, *NMR Biomed.* **22**: 148-157(2009). 7. Hum, Li, Tudorica, Oh, Hemmingson, Kettler, Grinstead, Laub, Springer, Huang, *Proc.Int Soc Magn Reson Med*.**19**: 3113 (2011).